Int J Clin Exp Med 2018;11(10):10562-10573
www.ijcem.com /ISSN:1940-5901/IJCEM0072433

Original Article

Summed score of initial chest radiograph and APACHE II preferably evaluates illness severity and accurately predicts ICU mortality in severe avian influenza H7N9

Wei Liu[1*], Wei Zhang[2*], Xiaosong Li[2*], Jin Lv[1*], Chao Tu[2], Liang Kang[2], Xiaoping Ma[2], Wenjuan Wu[2], Huisu Xia[2], Huidong Chen[3], Yuan Xiong[4*]

[1]Department of Interventional Radiology, [2]Intensive Care Unit, [3]Department of Endoscopy, Wuhan Medical Treatment Center, Wuhan, People's Republic of China; [4]College of Mathematics and Statistics, Hubei Engineering University, Xiaogan, People's Republic of China. [*]Equal contributors.

Received January 9, 2018; Accepted June 20, 2018; Epub October 15, 2018; Published October 30, 2018

Abstract: Objective: It is not rational to predict outcomes by chest imaging scores, regardless of illness severity, or to evaluate illness severity without considering imaging characteristics. Therefore, this study utilized a summed score of initial imaging and APACHE II/SOFA for evaluation of illness severity on ICU admission and prediction of ICU mortality in avian influenza (AI) H7N9. Methods: This retrospective study was conducted to record scores of radiographs, CT scans, APACHE II, SOFA, incidence of ARDS, multiple system organ failure (MSOF), and mortality. The aim of this study was to determine predictive accuracy and cut-off values of initial radiographic or CT scores (IRS/ICS), APACHE II, SOFA, (IRS/ICS + APACHE II), and (IRS/ICS + SOFA) and analyze correlation of each score to mortality in 22 patients with AI H7N9 at an ICU in Wuhan, China. Results: ARDS, MSOF, and mortality, respectively, occurred in 22 (100%), 17 (77.3%) and 10 (45.5%) patients. Cut-off values of (IRS + APACHE II), (IRS + SOFA), (ICS + APACHE II), and (ICS + SOFA) were 37.0, 28.0, 41.5 and 31.5, respectively, with sensitivity of 100%, 77.8%, 62.5%, and 62.5%, and specificity of 90.9%, 81.8%, 100% and 87.5% ($P < 0.001$, $P = 0.020$, 0.021, and 0.074). Mortality was positively correlated to (IRS + APACHE II), (IRS + SOFA), and (ICS + APACHE II) (P = 0.839, 0.534 and 0.597; all $P < 0.05$). Conclusion: The summed score of initial radiograph and APACHE II appears to be a preferable indicator for evaluation of illness severity on admission and for prediction of ICU mortality in AI H7N9.

Keywords: Avian influenza (AI) H7N9, radiography, computed tomography (CT), acute physiology and chronic health evaluation (APACHE) II score, sequential organ failure assessment (SOFA) score, mortality

Introduction

Since avian influenza (AI) H7N9 virus infection is a potentially fatal disease [1, 2], it is important to identify initial imaging findings as potential risk stratification to help triage patients, guide treatment, and monitor disease progression and treatment response. It may be indicative that more aggressive treatment and close monitoring of disease progression should be applied to patients with higher overall radiologic scores [2].

In a previous study conducted by Feng et al. [2] on chest imaging of patients with AI H7N9, chest radiographic and CT scores were assessed by determining the extent of patchy areas of ground-glass attenuation mixed with consolidation, which could be pathologically correlated with diffuse alveolar damage in lungs [2, 3]. However, there were some limitations in this study. It is not rational to predict clinical outcomes merely by initial imaging scores. Imaging severity is only one of numerous variables associated with illness severity and outcomes. Others include scores of acute physiology and chronic health evaluation (APACHE) and sequential organ failure assessment (SOFA). On the other hand, it is not reasonable to evaluate illness severity only by APACHE or SOFA scores, without considering imaging characteristics, as most clinicians previously have done.

Therefore, this study introduced an easier scoring method of evaluation of imaging findings in AI H7N9 and attempted to adopt a sum of initial imaging and illness severity scores (APACHE II

or SOFA) for a comprehensive evaluation of illness severity. Additionally, this study explored correlation of the summed score to incidence of MSOF and ICU mortality, utilizing the summed score for prediction of ICU mortality.

Materials and methods

This study is a retrospective review of clinical and chest imaging data obtained from 22 patients with laboratory-confirmed AI H7N9, hospitalized at the ICU of Wuhan Medical Treatment Center, China, from April 2015 to April 2017.

Ethics issues

This study complied with necessary ethical guidelines and was approved by the Research Ethics Board of Wuhan Medical Treatment Center. Informed consent was not required for this retrospective study.

Diagnostic criteria

AI H7N9 confirmed cases were defined according to positive test results for AI H7N9 viral RNA with pharyngeal swabs using reverse transcriptase polymerase chain reaction (RT-PCR), as described previously [4]. Mild or severe cases of H7N9 were defined as individuals with confirmed H7N9 virus infections that met the respiratory infection criteria, presenting with mild or severe respiratory symptoms and with or without any complications (including ARDS, shock, multi-organ failure, or hypoxemia) throughout the clinical course [5]. The objective index for severe cases was as follows: (1) X-rays showing lesions in multiple lobes or disease progression > 50% within 48 hours; (2) Dyspnea with a respiratory rate > 24 breaths per minute; (3) Hypoxemia with oxygen saturation ≤ 92% on oxygen at a flow rate of 3-5 L/minute; and (4) Shock, ARDS, or multiple organ dysfunction syndrome [6]. Accordingly, all 22 patients were identified as "severe" AI H7N9 cases.

Chest radiograph and CT scan

Chest radiographs were carried out by portable computed radiography at bedside with anteroposterior projection. All CT examinations were performed with patients in the supine position without administration of contrast material.

Scoring system

Chest radiographs and CT scans were assessed particularly for the presence and distribution of parenchymal abnormalities [7]. According to established knowledge, chest radiographic and CT findings included nodule or patchy opacity, fibrotic opacity, ground glass opacity (GGO), consolidation, air bronchograms, pleuritis, pleural effusion, and lymphadenopathy [2, 7]. GGO was defined as hazy areas of increased opacity or attenuation without concealing underlying vessels. Consolidation was defined as homogeneous opacification of the parenchyma obscuring underlying vessels. The extent of involvement of each abnormality was assessed independently for each of three zones: upper (above the carina), middle (below the carina and above the inferior pulmonary vein), and lower (below the inferior pulmonary vein) [2]. Reading radiologists used a standard 0 to 3 scoring system (0: no infiltration; 1: focal haziness or even small patchy lesion; 2: ground glass picture; 3: lobar consolidation), according to the severity of infiltration in each lung field (three lung fields in both right and left lungs). Scores were then added up to a total of 0-18 for assessment of each radiographic and CT film, as described by Hsu et al. [8].

Randomization and blindness

To avoid bias reading the chest radiologic films, radiologists were blinded to the information in terms of study procedures and patient clinical conditions, except for the knowledge that these were cases of AI H7N9 virus infection. Two radiologists reviewed and gave scores of the chest radiographs and CT scans, independently, with a final decision reached concerning findings by consensus when there was a discrepancy.

Evaluation of illness severity

APACHE II scores and SOFA scores were calculated for evaluation of illness severity on the day of admission to ICU in all patients, as previously depicted [9-11].

Interventions

All 22 patients were administered an antiviral regime, antibiotics, and methylprednisolone. Oxygen inhalation through a high-flow nasal oxygenator (Optiflow™) was used in 12 patients

Table 1. Comparison of demographics and baseline characteristics between survivors (*n* = 12) and non-survivors (*n* = 10)

Clinical Characteristic	Survivor (*n* = 12)	Non-survivor (*n* = 10)	Total (*n* = 22)	*p*
Gender, male, *n* (%)	6 (27.3)	9 (40.9)	15 (68.2)	0.452
Age, years				
Mean ± SD	45.8 ± 10.6	57.2 ± 18.6	51.0 ± 15.5	0.086
Median (IQR)	44.5 (38.5-54.5)	62.0 (44.8-72.3)	51.0 (39.5-65.3)	
Age distribution, n (%)				0.017
18-49	2 (9.1)	7 (31.8)	9 (40.9)	
50-64	3 (13.6)	5 (22.7)	8 (36.4)	
≥ 65	5 (22.7)	0 (0)	5 (22.7)	
Type of residence, *n* (%)				0.746
Urban	6 (27.3)	8 (36.4)	14 (63.6)	
Rural	4 (18.2)	4 (18.2)	8 (36.4)	
Occupation, *n* (%)				0.230
Worker	1 (4.5)	2 (9.1)	3 (13.6)	
Farmer	4 (18.2)	2 (9.1)	6 (27.3)	
Civil servant or company employee	1 (4.5)	3 (13.6)	4 (18.2)	
Retiree	2 (9.1)	0 (0)	2 (9.1)	
Individual operator	0 (0)	3 (13.6)	3 (13.6)	
Unemployed	2 (9.1)	2 (9.1)	4 (18.2)	
Smoker, *n* (%)	2 (9.1)	5 (22.7)	7 (31.8)	0.277
Alcohol consumer, *n* (%)	1 (4.5)	4 (18.2)	5 (22.7)	0.193
Pre-existing condition, *n* (%)	8 (66.7)	7 (70.0)	15 (68.2)	0.867
COPD	1 (4.5)	0 (0)	1 (4.5)	0.262
CCVD	4 (18.2)	4 (18.2)	8 (36.4)	0.746
Viral hepatitis	0 (0)	1 (4.5)	1 (4.5)	0.350
Chronic renal disease	1 (4.5)	0 (0)	1 (4.5)	0.262
Diabetes	1 (4.5)	2 (9.1)	3 (13.6)	0.650
Obesity	0 (0)	2 (9.1)	2 (9.1)	0.176
Postpartum	1 (4.5)	0 (0)	1 (4.5)	0.262
Previous surgery	3 (13.6)	7 (31.8)	10 (45.5)	0.184
Others	2 (9.1)	2 (9.1)	4 (18.2)	0.840
Exposure to poultry, *n* (%)	11 (50.0)	7 (31.8)	18 (81.8)	0.190
Incubation period, days (*n* = 8)				
Mean ± SD	5.5 ± 0.6	6.3 ± 4.6	5.9 ± 3.0	0.756
Median (IQR)	5.5 (5.0-6.0)	6 (2.0-10.8)	5.5 (5.0-6.8)	

Note: SD = standard deviation, IQR = interquartile range, COPD = chronic obstructive pulmonary disease, CCVD = cardio-cerebrovascular disease.

(54.5%). Non-invasive mechanical ventilator was adopted in nine patients (40.9%) and tracheal intubation and mechanical ventilation were executed in 14 patients (63.6%). Bronchoscopy was undertaken in seven patients (31.8%). Continuous venus-venus hemodiafiltration (CVVHDF) was given in ten patients (45.5%) for renal replacement or clearance of inflammatory cytokines. Extracorporeal membrane oxygenation (ECMO) treatment was performed in six patients (27.3%).

Complications and outcomes

Severe complications and clinical outcomes were recorded, including incidence of ARDS, multiple system organ failure (MSOF), and mortality during ICU stay, referring to diagnostic criteria [12, 13].

Data collection

Medical data from every patient were extracted and reviewed, including demographic details,

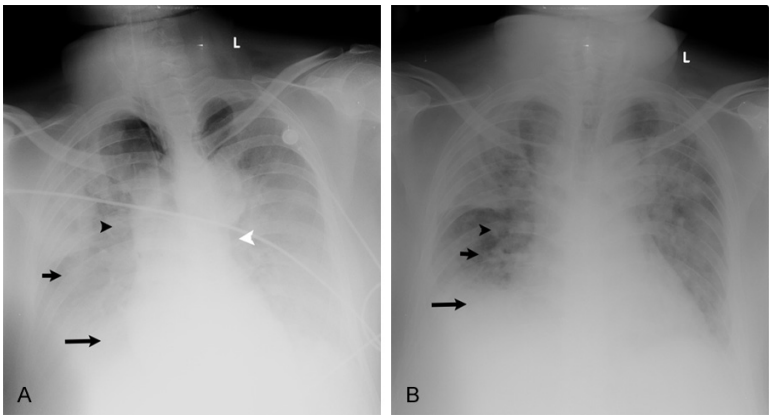

Figure 1. Anteroposterior chest radiographs obtained with portable bedside unit in a 38-year-old man with AI H7N9 from survival group show extensive bilateral infiltrates of patchy opacity (black arrowhead), GGO (short arrow), and consolidation (long arrow) in lower zone, and obscure hilum (white arrowhead) one day after ICU admission (10 days after symptom onset) (A), and decreased area of patchy opacity, GGO, and consolidation 15 days after ICU admission (i4 days after initial radiograph) (B). AI = Avian Influenza; GGO = ground glass opacity.

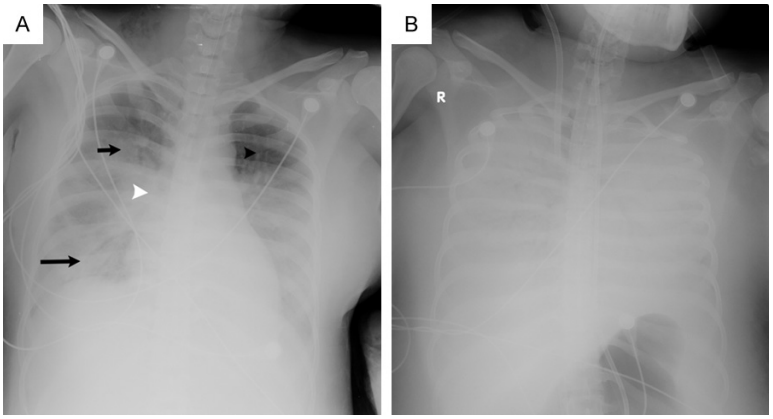

Figure 2. Anteroposterior chest radiographs obtained with portable bedside unit in a 25-year-old woman with AI H7N9 from non-survivor group show patchy opacities (black arrowhead) in upper zones, GGOs (short arrow) in middle zones, consolidation (long arrow) in lower zones and obscure hilum (white arrowhead) on both sides the right day on ICU admission (8 days after onset) (A), and complete whiteout on both sides 11 days after ICU admission (11 days after initial radiograph) (B). AI = Avian Influenza; GGO = ground glass opacity.

pre-existing conditions, exposure history, radiographic and CT findings, APACHE II and SOFA scores, severe complications, and clinical outcomes.

Statistical analysis

Continuous variables are expressed as mean ± standard deviations (SD) and median (interquartile range, IQR). Categorical variables are expressed as frequencies (percentages). Continuous variables were compared using independent-samples *t*-test. Differences between groups were evaluated by one-way analysis of variance (ANOVA). Pearson's Chi-square test or Fisher's exact test was used to compare categorical variables. Pearson's or Spearman's correlation analysis or Chi-square test was used and correlation coefficients (r, ρ, or φ) were calculated, as appropriate. The predictive accuracy of initial radiographic/CT scores (IRS/ICS), APACHE II scores, SOFA scores, and a summed score of initial imaging and APACHE II/SOFA (IRS/ICS + APACHE II/SOFA) for prediction of ICU mortality was analyzed. Area under the curve (AUC), sensitivity and specificity, and cut-off values were determined by their receiver operating characteristic (ROC) curves. All analyses were two-tailed and a p-value of < 0.05 was considered statistically significant. Statistical analyses were conducted using IBM SPSS Statistics version 19.0 (IBM Corp., Armonk, NY, USA).

Results

Demographic and epidemiological data

In the present study, there were no differences in gender, age, type of residence, occupation composition, smoking or drinking habits, pre-existing conditions, or history of exposure to poultry between survivors and non-survivors ($P > 0.05$), except that there was a higher percentage of patients aged 18-49 years old in non-survivors than in survivors ($P = 0.017$) (**Table 1**).

Radiologic features

Twenty patients (90.9%) underwent initial chest radiographs within 24 hours after admission to ICU and 21 (95.5%) received final ones within 48 hours before death or before discharge

Table 2. Pairwise comparisons of radiographic features between initials for survivors (*n* = 11), initials for non-survivors (*n* = 9), finals for survivors (*n* = 12) and finals for non-survivors (*n* = 9)

Radiographic Feature	Group 1 Initial for Survivor (*n* = 11)	Group 2 Initial for Non-survivor (*n* = 9)	Group 3 Final for Survivor (*n* = 12)	Group 4 Final for Non-survivor (*n* = 9)	*p*			
					Group 1 *vs.* Group 2	Group 3 *vs.* Group 4	Group 1 *vs.* Group 3	Group 2 *vs.* Group 4
Interval between symptom onset and radiograph								
Mean ± SD, days	7.7 ± 3.0	11.1 ± 6.5	19.0 ± 7.7	23.6 ± 12.4	0.140	0.350	< 0.001	0.020
Median (IQR), days	7.0 (6.0-10.0)	9.0 (8.5-10.5)	16.5 (14.3-20.8)	14.0 (14.0-36.0)				
Abnormality, *n* (%)								
Nodule or patchy opacity	10 (90.9)	9 (100)	11 (91.7)	9 (100)	0.353	0.375	0.949	NA
Fibrotic opacity	0 (0)	0 (0)	0 (0)	1 (11.1)	NA	0.237	NA	0.303
GGO	9 (81.8)	9 (100)	10 (83.3)	7 (77.8)	0.178	0.748	0.924	0.134
Consolidation	2 (18.2)	0 (0)	3 (25.0)	2 (22.2)	0.178	0.882	0.692	0.134
GGO and consolidation	3 (27.3)	0 (0)	3 (25.0)	2 (22.2)	0.089	0.882	0.692	0.134
Enlarged or obscure hilum	5 (45.5)	2 (22.2)	5 (41.7)	3 (33.3)	0.279	0.697	0.855	0.599
Pleuritis	6 (54.5)	6 (66.7)	6 (50.0)	5 (55.6)	0.582	0.801	0.827	0.629
Pleural effusion	4 (36.4)	2 (22.2)	6 (50.0)	4 (44.4)	0.492	0.801	0.510	0.317
Pulmonary edema	3 (27.3)	3 (33.3)	4 (33.3)	1 (11.1)	0.769	0.237	0.752	0.257
Atelectasis	1 (9.1)	1 (11.1)	3 (25.0)	1 (11.1)	0.881	0.422	0.315	1.000
Side distribution, *n* (%)								
Left	9 (81.8)	9 (100)	12 (100)	9 (100)	0.178	NA	0.122	NA
Right	10 (90.9)	9 (100)	12 (100)	9 (100)	0.353	NA	0.286	NA
Unilateral	1 (9.1)	0 (0)	0 (0)	0 (0)	0.353	NA	0.286	NA
Bilateral	9 (81.8)	9 (100)	12 (100)	9 (100)	0.178	NA	0.122	NA
Zone distribution, *n* (%)								
Right upper	8 (72.7)	8 (88.9)	10 (83.3)	9 (100)	0.369	0.198	0.538	0.303
Right middle	10 (90.9)	9 (100)	11 (91.7)	9 (100)	0.353	0.375	0.949	NA
Right lower	10 (90.9)	9 (100)	12 (100)	9 (100)	0.353	NA	0.286	NA
Left upper	7 (63.6)	8 (88.9)	9 (75.0)	8 (88.9)	0.194	0.422	0.554	1.000
Left middle	9 (81.8)	9 (100)	11 (91.7)	9 (100)	0.178	0.375	0.484	NA
Left lower	9 (81.8)	9 (100)	12 (100)	9 (100)	0.178	NA	0.122	NA
Radiographic score								
Mean ± SD	17.5 ± 7.2	19.0 ± 4.7	13.4 ± 4.2	25.0 ± 2.8	0.586	< 0.001	0.111	0.005
Median (IQR)	17.0 (16.0-22.0)	19.0 (18.0-21.0)	14.0 (11.0-17.0)	24.0 (24.0-27.0)				

Note: SD = standard deviation; IQR = interquartile range, GGO = ground glass opacity, NA = not available.

A

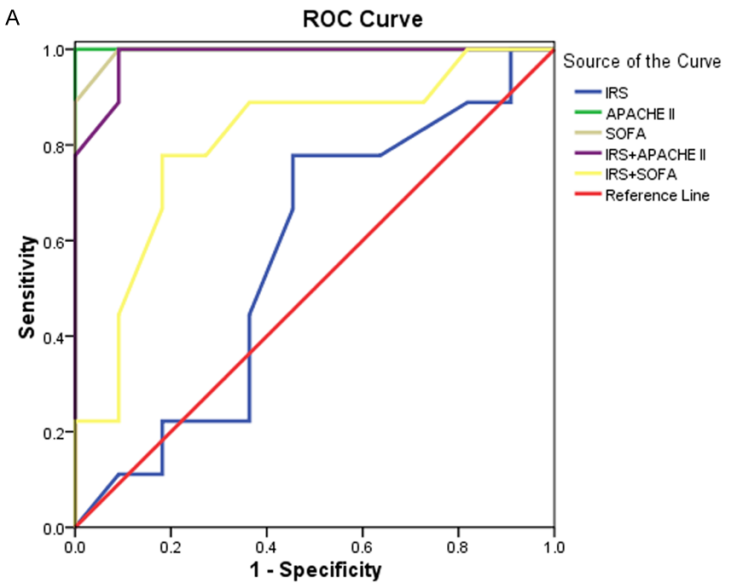

B

Variable	Cut-off	Sensitivity	Specificity	AUC	*p* value	95% CI	
						Lower bound	Upper bound
IRS	17.5	0.778	0.545	0.571	0.595	0.310	0.831
APACHE II	16.0	1.000	1.000	1.000	< 0.001	0.000	1.000
SOFA	6.5	1.000	0.909	0.995	< 0.001	0.000	1.000
IRS + APACHE II	37.0	1.000	0.909	0.985	< 0.001	0.000	1.000
IRS + SOFA	28.0	0.778	0.818	0.808	0.020	0.594	1.000

Figure 3. ROC curves (A) and accuracy analyses (B) for prediction of ICU mortality, indicating a cut-off value of 37.0 and 28.0 for (IRS + APACHE II) and (IRS + SOFA) with a sensitivity of 100% and 77.8%, and a specificity of 90.9% and 81.8%, respectively ($P < 0.001$ and $P = 0.020$). $N = 20$. ROC = receiver operating characteristic; IRS = initial radiographic score; APACHE = acute physiology and chronic health evaluation; SOFA = sequential organ failure assessment; AUC = area under curve; CI = confidence interval.

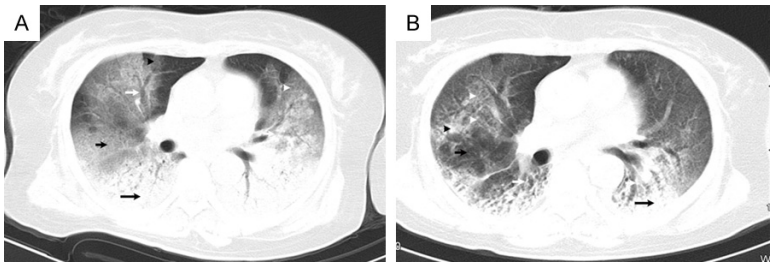

Figure 4. Axial CT images obtained in a 55-year-old woman with AI H7N9 from survival group show patchy opacity (black arrowhead), extensive GGO (short black arrow), and consolidation (long black arrow) appearing as a geographic pattern, reticulation (white arrowhead) superimposed on GGO, consolidation with air bronchograms (short white arrow) and extensive bilateral infiltrates predominantly in middle and lower zones 1 day after admission (7 days after onset) (A), and partial resorption of patchy opacity, GGO, consolidation, reticulation and air bronchograms 18 days after ICU admission (17 days after initial CT scan) (B). AI = Avian Influenza; GGO = ground glass opacity.

from ICU (**Figures 1** and **2**). Median interval between symptom onset and initial radiographs was 9.0 days (IQR, 7.0-10.0 days). Median interval between symptom onset and final radiographs was 15.0 days (IQR, 14.0-24.0 days). As **Table 2** exhibits, nodule or patchy opacity was the most common finding on both initial and final radiographs (95.0% and 95.2% of the radiographs, respectively). The 41 radiographs were divided into four groups according to different time phases (initial or final) or outcomes (survival or death). This study compared frequency, distribution, and scores of radiographic findings between the four groups. As **Table 2** shows, the mean score of final radiographs in non-survivors was statistically higher than that in survivors (25.0 *vs.* 13.4, $P < 0.001$), also statistically higher than the mean score of initial radiographs in non-survivors (25.0 *vs.* 19.0, $P = 0.005$). AUCs, sensitivity, specificity, and cut-off values of IRS, APACHE II, SOFA, (IRS + APACHE II), and (IRS + SOFA) for prediction of ICU mortality are manifested in **Figure 3**. As the figure shows, a cut-off value of 17.5 for IRS had sensitivity of 77.8% and specificity of 54.5% ($P = 0.595$) with an AUC of 0.571 [95% confidence interval (CI), 0.310-0.831], while a cut-off value of 37.0 and 28.0 for (IRS + APACHE II) and (IRS + SOFA) had sensitivity of 100% and 77.8% and specificity of 90.9% and 81.8%, respectively ($P < 0.001$ and $P = 0.020$).

CT findings

Initial CT scans were carried out in 16 patients (72.7%) a median of 7.0 days (IQR, 4.0-8.5 days) after symptom onset. Final ones were executed in ten patients (72.2%) a median of 17.0 days

Table 3. Comparison of initial CT features between survivors (*n* = 8) and non-survivors (*n* = 8), and of CT features in survivors between initials (*n* = 8) and finals (*n* = 9)

CT Feature	Group 1 Initial for Survivor (*n* = 8)	Group 2 Initial for Non-survivor (*n* = 8)	Group 3 Final for Survivor (*n* = 9)	*p*	
				Group1 *vs.* Group2	Group1 *vs.* Group3
Interval between onset and CT scan					
Mean ± SD, days	6.6 ± 2.7	5.8 ± 2.9	21.3 ± 12.8	0.545	0.006
Median (IQR), days	7.5 (4.5-8.5)	5.5 (4.0-8.5)	17.0 (15.0-24.0)		
Abnormality, *n* (%)					
Nodule or patchy opacity	7 (87.5)	6 (75.0)	9 (100)	0.522	0.274
Funicular opacity	3 (37.5)	0 (0)	4 (44.4)	0.055	0.772
Air bronchograms	3 (37.5)	5 (62.5)	6 (66.7)	0.317	0.229
Atelectasis	0 (0)	1 (12.5)	2 (22.2)	0.302	0.156
Pleuritis	7 (87.5)	6 (75.0)	8 (88.9)	0.522	0.929
Pleural effusion	2 (25.0)	4 (50.0)	3 (33.3)	0.302	0.707
Hilar lymphadenopathy	0 (0)	3 (37.5)	0 (0)	0.055	NA
GGO	4 (50.0)	7 (87.5)	8 (88.9)	0.106	0.079
Consolidation	6 (75.0)	7 (87.5)	8 (88.9)	0.522	0.453
GGO and consolidation	4 (50.0)	6 (75.0)	7 (77.8)	0.302	0.232
Side distribution, *n* (%)					
Left	6 (75.0)	6 (75.0)	9 (100)	1.000	0.110
Right	8 (100)	7 (87.5)	9 (100)	0.302	NA
Unilateral	2 (25.0)	3 (37.5)	0 (0)	0.590	0.110
Bilateral	6 (75.0)	5 (62.5)	9 (100)	0.590	0.110
Zone distribution, *n* (%)					
Right upper	7 (87.5)	5 (62.5)	9 (100)	0.248	0.274
Right middle	6 (75.0)	5 (62.5)	8 (88.9)	0.590	0.453
Right lower	8 (100)	7 (87.5)	9 (100)	0.302	NA
Left upper	4 (50.0)	5 (62.5)	7 (77.8)	0.614	0.232
Left middle	5 (62.5)	6 (75.0)	8 (88.9)	0.590	0.200
Left lower	6 (75.0)	4 (50.0)	9 (100)	0.302	0.110
CT score					
Mean ± SD	14.5 ± 10.8	19.8 ± 10.9	16.9 ± 4.6	0.350	0.576
Median (IQR)	11.5 (6.0-24.5)	24.0 (9.0-29.0)	15.0 (14.0-21.0)		

Note: SD = standard deviation, IQR = interquartile range, GGO = ground glass opacity, NA = not available.

(IQR, 15.0-24.0 days) following symptom onset (**Figure 4**). As **Table 3** shows, nodule or patchy opacity, pleuritis, and consolidation were equally the most common findings on initial chest CT scans (13/16, 81.3%). Nodule or patchy opacity was the most frequent finding on final CT scans (10/10, 100%). Similarly, 25 CT scans were divided into three groups according to diverse time phases and outcomes. This study compared frequency, distribution, and scores of lung findings on CT scans between the three groups. One final CT scan on a non-survivor was exempt from comparison due to small sample size. As **Table 3** displays, there were not any substantial differences with respect to frequency, distribution, or scores of CT findings between non-survivors and survivors on initial CT scans, or between initial CT scans and final CT scans in survivors (all $P > 0.05$). AUCs, sensitivity, specificity, and cut-off values of ICS, APACHE II, SOFA, (ICS + APACHE II), and (ICS + SOFA) for prediction of ICU mortality are presented in **Figure 5**. As the figure shows, a cut-off value of 27.0 for ICS had sensitivity of 50.0% and specificity of 87.5% ($P = 0.401$) with an AUC of 0.625 (95% CI, 0.337-0.913), while cut-off values of 41.5 and 31.5 for (ICS + APAHE II) and (ICS + SOFA) had sensitivity of 62.5% and 62.5% and specificity of 100% and 87.5%, respectively ($P = 0.021$ and 0.074).

Complications and outcomes

Ten patients (45.5%) died, while the other 12 survived and were discharged from ICU. Non-survivors had an appreciably higher percent-

A

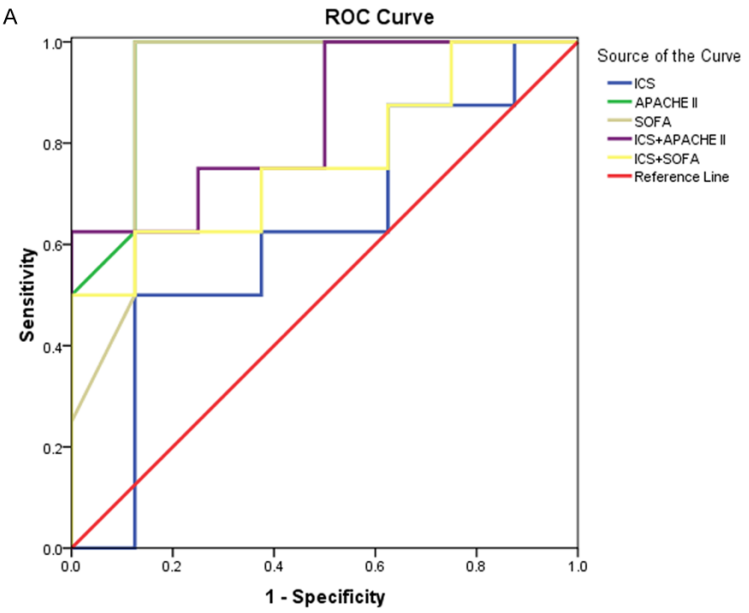

B

Variable	Cut-off	Sensitivity	Specificity	AUC	*p* value	95%CI	
						Lower bound	Upper bound
ICS	27.0	0.500	0.875	0.625	0.401	0.337	0.913
APACHE II	16.0	1.000	0.875	0.945	0.003	0.000	1.000
SOFA	6.5	1.000	0.875	0.922	0.005	0.000	1.000
ICS + APACHE II	41.5	0.625	1.000	0.844	0.021	0.000	1.000
ICS + SOFA	31.5	0.625	0.875	0.766	0.074	0.517	1.000

Figure 5. ROC curves (A) and accuracy analyses (B) for prediction of ICU mortality, demonstrating a cut-off value of 41.5 and 31.5 for (ICS + APAHE II) and (ICS + SOFA) with a sensitivity of 62.5% and 62.5%, and a specificity of 100% and 87.5%, respectively (*P* = 0.021 and 0.074). N = 16. ROC = receiver operating characteristic; ICS = initial CT score; APACHE = acute physiology and chronic health evaluation; SOFA = sequential organ failure assessment = AUC, area under curve; CI = confidence interval.

age of patients with mechanical ventilation required (100% *vs.* 50%, *P* = 0.009), MSOF incidence (100% *vs.* 58.3%, *P* = 0.020), mean APACHE II (24.6 *vs.* 9.3, *P* < 0.001), and mean SOFA score (11.4 *vs.* 4.6, *P* < 0.001) than survivors (**Table 4**).

Correlation

Correlation analyses, as shown in **Table 5**, revealed a positive correlation of (1) APACHE II, SOFA, and (IRS + APACHE II) to MSOF incidence (P = 0.582, 0.476 and 0.552; *P* = 0.007, 0.034 and 0.012), (2) APACHE II, SOFA, (IRS + APACHE II), and (IRS + SOFA) to ICU mortality (P = 0.864, 0.864, 0.839 and 0.534; *P* < 0.001, *P* < 0.001, *P* < 0.001, and *P* = 0.015), (3) frequency of left upper zone involved and APACHE II to MSOF incidence (φ = 0.545, P = 0.539; *P* = 0.035 and 0.031), and (4) APACHE II, SOFA, and (ICS + APACHE II) to ICU mortality (P = 0.774, 0.738 and 0.597; *P* < 0.001, *P* = 0.001 and 0.015).

Discussion

In the present study, demographics, pre-existing conditions, and history of exposure to poultry were comparable between survivors and non-survivors. Thus, there were not any confounding factors originating from demographic and epidemiological characteristics that potentially influenced comparisons of imaging and illness severity between survivors and non-survivors.

Regarding the imaging scoring system, Soepandi et al. [10] used a crude classification of chest X-ray (CXR) findings by simply categorizing the degree of consolidation as > 50% or not and whether consolidation was unilateral or bilateral. This type of system may be helpful to busy clinicians but lacks the finesse of imaging characteristics. In Feng et al.'s scoring system [2], the location of lesions was additionally defined as peripheral or central, as well as upper, middle, or lower. Accordingly, a total of twelve lung zones in each patient were subjected to radiograph and CT assessment. Moreover, all lesions in each lung zone were scaled to the extent of affected parenchyma according to the percentage of abnormal lung. These complex procedures are undoubtedly unsuitable for busy physicians and radiologists in emergency settings. This study came across a scoring method developed by the same principle for radiographic and CT scoring as Feng et al. and used in a clinical study on SARS by Hsu et al. [8]. This method was much easier to perform than that used by Feng et al. Thus, this study attempted to introduce this easier scoring method into evaluation of radiographic and CT features for AI H7N9.

In comparison, it was found that mean scores of final radiographs in non-survivors were near-

Table 4. Comparison of incidence of ARDS and MSOF, and APACHE II and SOFA scores between survivors (*n* = 12) and non-survivors (*n* = 10)

	Survivor (*n* = 12)	Non-survivor (*n* = 12)	Total (*n* = 22)	*p*
Complication				
ARDS	12 (100)	10 (100)	22 (100)	NA
Mechanical ventilation required	6 (50.0)	10(100)	16 (72.7)	0.009
MSOF	7 (58.3)	10 (100)	17 (77.3)	0.020
APACHE II score				
Mean ± SD	9.3 ± 5.6	24.6 ± 5.2	16.2 ± 9.4	< 0.001
Median (IQR)	7.5 (6.0-12.0)	23.0 (19.8-30.3)	16.0 (7.0-23.0)	
SOFA score				
Mean ± SD	4.6 ± 1.4	11.4 ± 2.4	7.7 ± 3.9	< 0.001
Median (IQR)	4.0 (4.0-5.0)	11.5 (9.8-12.5)	7.0 (4.0-11.0)	

Note: ARDS = acute respiratory distress syndrome, MSOF = multiple systems organ failure, APACHE = acute physiology and chronic health evaluation, SOFA = sepsis organ-related failure assessment, SD = standard deviation, IQR = interquartile, NA = not available.

ly twice as high as that in survivors. It was also found that mean scores of final radiographs were much higher than that of initial radiographs in non-survivors. These results implied that patients with mortal outcomes had more diffuse and progressive alveolar damage than those with survival outcomes, which were pathologically correlated with consolidation and GGO [2, 3] and contributive to hypoxemia [1, 2]. Unlike radiographic scores, there were no appreciable differences concerning scores of CT features between initial and final CT scans in survivors or between survivors and non-survivors on initial CT scans. This lack of statistical significance could be, in part, attributed to the small size of sample in patients receiving initial and final CT scans.

Avian influenza progresses rapidly to severe pneumonia, ARDS, and respiratory failure, resulting in the requirement for ICU admission and mechanical ventilation. It may also lead to development of acute kidney injury, shock, MSOF, and even death [1, 2, 7, 14-16]. ARDS reflects the severity of respiratory failure [2, 17]. It is considered as a strong predictor of mortality [2, 17] since the development of ARDS has consistently been shown to be associated with fatal outcomes in avian influenza [15, 18]. However, correlation of ARDS to ICU mortality could not be analyzed because all 22 patients in the present study had already developed ARDS on admission to CU. APACHE II and SOFA scores are well-acknowledged indicators for evaluation of acute physiology, chronic health, and sequential organ failure. They may be helpful in identifying at-risk patients on ICU admission [10, 11]. In the present study, the mean score of SOFA and APACHE II on admission was apparently higher in patients with mortal outcomes than in those with opposite outcomes. This has been consistently reported in previous studies in patients with AI H7N9 or AI H5N1 [10, 19]. Correlation analyses unveiled a moderate positive correlation of summed score of initial imaging and APACHE II to incidence of MSOF or ICU mortality, with correlation coefficients approximately equal to or slightly lower than that of APACHE II. Using a grading method, scores at initial chest radiographs and CT images had significance in prediction of clinical outcomes [2].

Regarding prediction of ICU mortality, this study produced a cutoff value of 17.5 and 27 for an initial radiographic and CT scores, respectively. The cut-off value and sensitivity of initial radiographic scores and specificity of the cut-off value of initial CT scores were similar to that in the study by Feng et al.. However, it is still not rational to predict clinical outcomes merely by initial imaging scores in that imaging severity is only one of numerous variables assessing illness severity and influenced outcomes. Other indicators, such as APACHE or SOFA scores, ought to be considered. Merely taking prognostic value into account, initial APACHE and SOFA scores are two optimal predictive indicators relying on their sensitivity and specificity of approximate 100%. Despite the indispensable role of chest imaging in assessment of illness severity and progression, APACHE or SOFA scor-

Table 5. Correlation of initial radiographic (n = 20) and CT features (n = 16) to MSOF incidence and ICU mortality

Initial Radiographic Feature (n = 20)	MSOF Incidence		ICU Mortality		Initial CT Feature (n = 16)	MSOF Incidence		ICU Mortality	
	Correlation Coefficient	p	Correlation Coefficient	p		Correlation Coefficient	p	Correlation Coefficient	p
Abnormality					Abnormality				
Nodule or patchy opacity	-0.132	0.564	0.208	0.366	Nodule or patchy opacity	-0.231	0.371	-0.160	0.535
GGO	0.192	0.402	0.302	0.189	GGO	0.022	0.933	0.405	0.117
Consolidation	-0.192	0.402	-0.302	0.189	Consolidation	0.179	0.487	0.160	0.535
GGO and consolidation	-0.192	0.402	-0.302	0.189	GGO and consolidation	-0.041	0.873	0.258	0.317
Pleuritis	0.236	0.304	0.123	0.592	Pleuritis	0.179	0.487	-0.160	0.535
Pleural effusion	-0.378	0.099	-0.154	0.503	Pleural effusion	0.372	0.150	0.258	0.317
Fibrotic opacity	NA	NA	NA	NA	Fibrotic opacity	-0.179	0.487	-0.480	0.063
Atelectasis	-0.192	0.402	0.034	0.884	Atelectasis	0.124	0.631	0.258	0.317
Enlarged or obscure hilum	-0.303	0.187	-0.242	0.291	Hilar lymphadenopathy	0.231	0.371	0.480	0.063
Pulmonary edema	0.126	0.583	0.066	0.774	Air bronchograms	-0.160	0.535	0.250	0.333
Side distribution					Side distribution				
Left	0.192	0.402	0.302	0.189	Left	0.092	0.720	< 0.001	1.000
Right	-0.132	0.564	0.208	0.366	Right	-0.124	0.631	-0.258	0.317
Unilateral	-0.397	0.083	-0.208	0.366	Unilateral	-0.022	0.933	0.135	0.602
Bilateral	0.192	0.402	0.302	0.189	Bilateral	0.022	0.933	-0.135	0.602
Zone distribution					Zone distribution				
Right upper	0.000	1.000	0.201	0.381	Right upper	0.092	0.720	-0.289	0.264
Right middle	-0.132	0.564	0.208	0.366	Right middle	0.022	0.933	-0.135	0.602
Right lower	-0.132	0.564	0.208	0.366	Right lower	-0.124	0.631	-0.258	0.317
Left upper	0.200	0.383	0.290	0.206	Left upper	0.545	0.035	0.126	0.626
Left middle	0.192	0.402	0.302	0.189	Left middle	0.367	0.155	0.135	0.602
Left lower	0.192	0.402	0.302	0.189	Left lower	-0.041	0.873	-0.258	0.317
Imaging or clinical score					Imaging or clinical score				
IRS	0.201	0.395	0.123	0.607	ICS	0.261	0.329	0.217	0.419
APACHE II	0.582	0.007	0.864	< 0.001	APACHE II	0.539	0.031	0.774	< 0.001
SOFA	0.476	0.034	0.864	< 0.001	SOFA	0.473	0.064	0.738	0.001
IRS + APACHE II	0.552	0.012	0.839	< 0.001	ICS + APACHE II	0.435	0.093	0.597	0.015
IRS + SOFA	0.372	0.106	0.534	0.015	ICS + SOFA	0.400	0.125	0.461	0.072

Note: MSOF = multiple systems organ failure, GGO = ground glass opacity, IRS = initial radiographic score, ICS = initial CT score, APACHE = acute physiology and chronic health evaluation, SOFA = sequential organ failure assessment, NA = not available.

ing systems consist of no radiographic or CT components and, thus, are far from being considered adequate and ideal. Therefore, it is necessary and urgent that a series of indicators be developed for comprehensive evaluation of illness severity as well as precise prediction of clinical outcomes.

Approvingly, a summed score of initial radiograph and APACHE II met both expectations above. It reflected the frequency and distribution of such radiographic characteristics as GGO and consolidation pathologically associated with alveolar injury and anoxia, while having potent prognostic power for ICU mortality. ROC analyses revealed that this combined score had a much more competent performance in prediction of ICU mortality than a single radiographic score. Due to its positive correlation to ICU mortality, this combined score can function as a better indicator for both evaluation of illness severity and prediction of outcomes.

This study concludes that a summed score of initial radiograph and APACHE II demonstrates high sensitivity and specificity in prediction of ICU mortality, with strong positive correlation to ICU mortality. This combined score is a preferable indicator for comprehensive evaluation of illness severity on admission and for accurate prediction of ICU mortality in AI H7N9 patients. If applied in clinical practice with larger sample sizes, this novel scoring method may shed new light regarding better clinical evaluation and management, possibly leading to even better outcomes for this globally life-threatening disease.

Disclosure of conflict of interest

None.

Address correspondence to: Huisu Xia, Intensive Care Unit, Wuhan Medical Treatment Center, 1 Yintan Road, Dongxihu District, Wuhan 430023, Hubei Province, People's Republic of China. Tel: +86-27-85509963; Fax: +86-27-85509005; E-mail: xiahs0816@yeah.net; Huidong Chen, Department of Endoscopy, Wuhan Medical Treatment Center, 1 Yintan Road, Dongxihu District, Wuhan 430023, Hubei Province, People's Republic of China. E-mail: 18986055160@163.com

References

[1] Gao HN, Lu HZ, Cao B, Du B, Shang H, Gan JH, Lu SH, Yang YD, Fang Q, Shen YZ, Xi XM, Gu Q, Zhou XM, Qu HP, Yan Z, Li FM, Zhao W, Gao ZC, Wang GF, Ruan LX, Wang WH, Ye J, Cao HF, Li XW, Zhang WH, Fang XC, He J, Liang WF, Xie J, Zeng M, Wu XZ, Li J, Xia Q, Jin ZC, Chen Q, Tang C, Zhang ZY, Hou BM, Feng ZX, Sheng JF, Zhong NS and Li LJ. Clinical findings in 111 cases of influenza A (H7N9) virus infection. N Engl J Med 2013; 368: 2277-2285.

[2] Feng F, Jiang Y, Yuan M, Shen J, Yin H, Geng D, Xu J, Hua Y, Shi J, Shi Y and Zhang Z. Association of radiologic findings with mortality in patients with avian influenza H7N9 pneumonia. PLoS One 2014; 9: e93885.

[3] Marchiori E, Zanetti G, Fontes CA, Santos ML, Valiante PM, Mano CM, Teixeira GH and Hochhegger B. Influenza A (H1N1) virus-associated pneumonia: high-resolution computed tomography-pathologic correlation. Eur J Radiol 2011; 80: e500-504.

[4] Dai J, Zhou X, Dong D, Liu Y, Gu Q, Zhu B, Wu C and Cai H. Human infection with a novel avian-origin influenza A (H7N9) virus: serial chest radiographic and CT findings. Chin Med J (Engl) 2014; 127: 2206-2211.

[5] Qin Y, Horby PW, Tsang TK, Chen E, Gao L, Ou J, Nguyen TH, Duong TN, Gasimov V, Feng L, Wu P, Jiang H, Ren X, Peng Z, Li S, Li M, Zheng J, Liu S, Hu S, Hong R, Farrar JJ, Leung GM, Gao GF, Cowling BJ and Yu H. Differences in the epidemiology of human cases of avian influenza A (H7N9) and A (H5N1) viruses infection. Clin Infect Dis 2015; 61: 563-571.

[6] Li Q, Zhou L, Zhou M, Chen Z, Li F, Wu H, Xiang N, Chen E, Tang F, Wang D, Meng L, Hong Z, Tu W, Cao Y, Li L, Ding F, Liu B, Wang M, Xie R, Gao R, Li X, Bai T, Zou S, He J, Hu J, Xu Y, Chai C, Wang S, Gao Y, Jin L, Zhang Y, Luo H, Yu H, He J, Li Q, Wang X, Gao L, Pang X, Liu G, Yan Y, Yuan H, Shu Y, Yang W, Wang Y, Wu F, Uyeki TM and Feng Z. Epidemiology of human infections with avian influenza A (H7N9) virus in China. N Engl J Med 2014; 370: 520-532.

[7] Wang Q, Zhang Z, Shi Y and Jiang Y. Emerging H7N9 influenza A (novel reassortant avian-origin) pneumonia: radiologic findings. Radiology 2013; 268: 882-889.

[8] Hsu CH, Hwang KC, Chao CL, Chang SG, Ho MS, Lin JG, Chang HH, Kao ST, Chen YM and Chou P. An evaluation of the additive effect of natural herbal medicine on SARS or SARS-like infectious diseases in 2003: a randomized, double-blind, and controlled pilot study. Evid Based Complement Alternat Med 2008; 5: 355-362.

[9] Knaus WA, Draper EA, Wagner DP and Zimmerman JE. APACHE II: a severity of disease classification system. Crit Care Med 1985; 13: 818-829.

[10] Soepandi PZ, Burhan E, Mangunnegoro H, Nawas A, Aditama TY, Partakusuma L, Isbaniah F,

Ikhsan M, Swidarmoko B, Sutiyoso A, Malik S, Benamore R, Baird JK and Taylor WR. Clinical course of avian influenza A(H5N1) in patients at the persahabatan hospital, Jakarta, Indonesia, 2005-2008. Chest 2010; 138: 665-673.

[11] Vincent JL, de Mendonca A, Cantraine F, Moreno R, Takala J, Suter PM, Sprung CL, Colardyn F and Blecher S. Use of the SOFA score to assess the incidence of organ dysfunction/failure in intensive care units: results of a multicenter, prospective study. Working group on "sepsis-related problems" of the European society of intensive care medicine. Crit Care Med 1998; 26: 1793-1800.

[12] Ranieri VM, Rubenfeld GD, Thompson BT, Ferguson ND, Caldwell E, Fan E, Camporota L and Slutsky AS. Acute respiratory distress syndrome: the Berlin definition. JAMA 2012; 307: 2526-2533.

[13] Pinsky MR and Matuschak GM. Multiple systems organ failure: failure of host defense homeostasis. Crit Care Clin 1989; 5: 199-220.

[14] Chi Y, Zhu Y, Wen T, Cui L, Ge Y, Jiao Y, Wu T, Ge A, Ji H, Xu K, Bao C, Zhu Z, Qi X, Wu B, Shi Z, Tang F, Xing Z and Zhou M. Cytokine and chemokine levels in patients infected with the novel avian influenza A (H7N9) virus in China. J Infect Dis 2013; 208: 1962-1967.

[15] Qureshi NR, Hien TT, Farrar J and Gleeson FV. The radiologic manifestations of H5N1 avian influenza. J Thorac Imaging 2006; 21: 259-264.

[16] Belser JA, Bridges CB, Katz JM and Tumpey TM. Past, present, and possible future human infection with influenza virus A subtype H7. Emerg Infect Dis 2009; 15: 859-865.

[17] So LK, Lau AC, Yam LY, Cheung TM, Poon E, Yung RW and Yuen KY. Development of a standard treatment protocol for severe acute respiratory syndrome. Lancet 2003; 361: 1615-1617.

[18] Chotpitayasunondh T, Ungchusak K, Hanshaoworakul W, Chunsuthiwat S, Sawanpanyalert P, Kijphati R, Lochindarat S, Srisan P, Suwan P, Osotthanakorn Y, Anantasetagoon T, Kanjanawasri S, Tanupattarachai S, Weerakul J, Chaiwirattana R, Maneerattanaporn M, Poolsavathitikool R, Chokephaibulkit K, Apisarnthanarak A and Dowell SF. Human disease from influenza A (H5N1), Thailand, 2004. Emerg Infect Dis 2005; 11: 201-209.

[19] Yang M, Gao H, Chen J, Xu X, Tang L, Yang Y, Liang W, Yu L, Sheng J and Li L. Bacterial coinfection is associated with severity of avian influenza A (H7N9), and procalcitonin is a useful marker for early diagnosis. Diagn Microbiol Infect Dis 2016; 84: 165-169.